Spatial-Correlation-Based Error Weighting Method for Efficient Application of Filtered Reference Algorithm in Multichannel Active Noise Control

Meiling Hu*†, Jing Lu‡ and Qingyu Ma*§
* School of Computer and Electronic Information, Nanjing Normal University, China
† Ministry of Education Key Laboratory of NSLSCS, Nanjing Normal University, China
‡ Key Laboratory of Modern Acoustics and Institute of Acoustics, Nanjing University, China
§ Taizhou College of Nanjing Normal University, China
E-mail: humeiling@nnu.edu.cn, lujing@nju.edu.cn, maqingyu@njnu.edu.cn

***Abstract*—A multichannel active noise control (ANC) system with multiple secondary sources and error microphones is necessary for spatial ANC, which has raised a major challenge for the real-time implementation of the ANC system since the computational complexity increases with the number of reference signals, secondary sources, and error microphones. Typical methods to mitigate the complexity are decentralized algorithms and distributed algorithms. Decentralized algorithms suffer from stability issues, and the distributed algorithms require reliable data communication. In this paper, we propose a weighted error method to reduce the required number of error microphones used in real-time processing. The method is based on the spatial similarity of sound pressures in a constrained region. Thus, the overall sound pressure can be given by the weighted sum of several error microphones. Our results demonstrate that even using only one error microphone in the real-time processing, the proposed method achieves noise reduction levels comparable to the centralized approach with less than 1.5 dB degradation while offering significant computational savings. Furthermore, as the number of employed microphones increases, the noise reduction performance of our method improves accordingly.**

I. Introduction

Multichannel active noise control (ANC) system employing multiple secondary sources and error microphones is widely applied in environments such as automobile cabins [1], and windows [2]. Centralized algorithms, notably the filtered reference least mean squares (FxLMS) and filtered error least mean squares (FeLMS), are commonly used in multichannel ANC. While these centralized algorithms achieve the best noise reduction performance and exhibit fast convergence, their computational complexity, which scales with the number of reference signals, secondary sources, and error microphones [3] poses a significant implementation challenge. Although FeLMS is more computationally efficient than FxLMS for ANC systems with multiple references, this advantage diminishes for the system of only a single reference [4].

Frequency-domain [5] and subband-domain [6], [7] methods are commonly applied to reduce computational complexity in ANC. Decentralized [8]–[10] and distributed [11], [12] methods are designed specifically for multichannel ANC for computational saving purposes. Decentralized algorithms partition the ANC system into multiple independent control subsystems, each with fewer secondary sources and errors to ease the computational burden [13]. However, this approach risks the system stability and also usually sacrifices the noise reduction performance [9], [14], [15]. Compared to decentralized ANC, distributed ANC requires inter-node communication and imposes constraints on the similarity among the control filters across subsystems [16]. The incremental strategy for distributed ANC updates the control filters with a single error microphone in a circle. While computations are distributed across multiple processing units, the total computational load is not reduced compared to centralized approaches [17]. Data communication is essential for the incremental strategy, but the communication is vulnerable to the failure of a single node because of the fixed simple cyclic linking path. In contrast, the single-task diffusion strategy enhances robustness against link failures through the diverse linking paths [18] at the expense of higher computation complexity than the incremental strategy. The multitask diffusion FxLMS can effectively reduce the total computational complexity [19], but the algorithm enforces strong similarity among control filters and thus sacrifices the stability and noise reduction performance. The augmented diffusion FxLMS improves the performance of the multitask diffusion FxLMS by allowing different estimates of control filters across nodes [11] at a price of increased computational load and communication delays between nodes compared to the multitask diffusion FxLMS. Moreover, the augmented diffusion FxLMS raises a neighbor nodes partitioning strategy problem.

Decentralized and distributed methods decrease the computation complexity by breaking the ANC system into multiple independent or dependent subsystems with fewer secondary sources and error microphones. In [20], several error microphones are activated at a time and switched randomly or sequentially to reduce the computational cost. Although the method shows effectiveness for low-frequency tonal noise of

This research is supported by the National Natural Science Foundation of China (Grant No. 12404537), Natural Science Foundation of Jiangsu Province (No. BE2022814), and the Ministry of Education Key Laboratory of NSLSCS.

979-8-3315-7206-8/25/$31.00

vibrating casings, it considers each set of error microphones as independent, and just like the decentralized system, it might cause instability for a more complicated system. Instead of considering very error microphone as independent, in this paper, the spatial correlation among error microphones is utilized to reduce the number of employed error microphones, and thus reduces the computing effort. Spatial correlation of sound pressure is widely utilized in virtual sensing techniques [21]–[25], which means that sound pressures within a limited distance are correlated. The correlation suggests that precise control of every error microphone in a spatial region may be unnecessary. Instead, spatial control can be achieved using a weighted sum of the error signals from a subset of microphones. The subset of active microphones is periodically and randomly selected so that information contained in all microphones can be utilized. Compared to centralized algorithms, the proposed method can save significant computational effort at the expense of acceptable noise reduction performance degradation. Compared to the decentralized method, the proposed method does not show instability issues. Compared to the distributed method, the proposed method avoids data communication between processors.

II. Method

A. Formulation of the Multichannel ANC System

Without loss of generality, a multichannel ANC system with a single reference is considered in this paper. A schematic diagram of the multichannel ANC system combined with the error-weighting method is shown in Fig. 1, where x represents the reference signal, y_l (l=1, 2, …, L) is the output of the adaptive filter. The error signals captured by the error microphones are denoted as e_m (m=1, 2, …, M), which are then weighted to generate Q channels of signals for control filters updating. The secondary path between the m-th error microphone and the l-th secondary source is represented by the column vector $\mathbf{s}_{ml}$ with the length of J, and the l-th control filter is represented by the column vector $\mathbf{w}_l$ with the length of N.

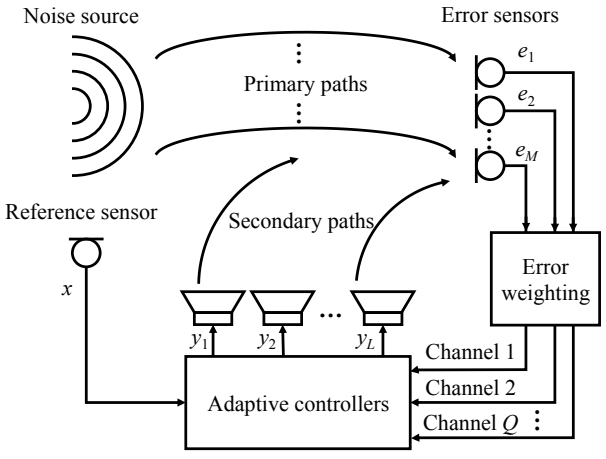

Fig. 1. Illustration of a multichannel ANC system.

The reference signal vector of length N is defined as

$$\mathbf{x}_N(n) = \begin{bmatrix} x(n) & x(n-1) & \cdots & x(n-N+1) \end{bmatrix}^{\mathrm{T}}. \quad (1)$$

Let $y_l(n)$ be the output vector of the l-th secondary source with the length of J, that is

$$\mathbf{y}_l(n) = \begin{bmatrix} y_l(n) & y_l(n-1) & \cdots & y_l(n-J+1) \end{bmatrix}^{\mathrm{T}}, \quad (2)$$

where $y_l(n) = \mathbf{x}_N^{\mathrm{T}}(n)\,\mathbf{w}_l(n)$. The n-th error signal at the m-th error microphone can then be represented by

$$e_m(n) = d_m(n) + \mathbf{s}_{m1}^{\mathrm{T}}\mathbf{y}_1(n) + \cdots + \mathbf{s}_{mL}^{\mathrm{T}}\mathbf{y}_L(n), \quad (3)$$

where $d_m(n)$ is the n-th disturbance noise signal at the m-th error microphone. Vectorizing the above equation, we have

$$\underbrace{\begin{bmatrix} e_1(n) \\ \vdots \\ e_M(n) \end{bmatrix}}_{\mathbf{e}(n)} = \underbrace{\begin{bmatrix} d_1(n) \\ \vdots \\ d_M(n) \end{bmatrix}}_{\mathbf{d}(n)} + \underbrace{\begin{bmatrix} \mathbf{s}_{11} & \cdots & \mathbf{s}_{M1} \\ \vdots & \ddots & \vdots \\ \mathbf{s}_{1L} & \cdots & \mathbf{s}_{ML} \end{bmatrix}^{\mathrm{T}}}_{\mathbf{S}} \underbrace{\begin{bmatrix} \mathbf{y}_1(n) \\ \vdots \\ \mathbf{y}_L(n) \end{bmatrix}}_{\mathbf{y}(n)}. \quad (4)$$

With the notation used in the equation, we have

$$\mathbf{e}(n) = \mathbf{d}(n) + \mathbf{S}^{\mathrm{T}}\mathbf{y}(n). \quad (5)$$

Denoting

$$\mathbf{X}(n) = \begin{bmatrix} \mathbf{x}_N(n) & \mathbf{x}_N(n-1) & \cdots & \mathbf{x}_N(n-J+1) \end{bmatrix}^{\mathrm{T}} \quad (6)$$

with a dimension of $J \times N$, then $\mathbf{y}_l(n) = \mathbf{X}(n)\,\mathbf{w}_l(n)$. Denoting

$$\mathbf{y}(n) = \begin{bmatrix} \mathbf{y}_1(n) \\ \vdots \\ \mathbf{y}_L(n) \end{bmatrix} = \underbrace{\begin{bmatrix} \mathbf{X}(n) & & \mathbf{0} \\ & \ddots & \\ \mathbf{0} & & \mathbf{X}(n) \end{bmatrix}}_{\mathbf{X}_+(n)} \underbrace{\begin{bmatrix} \mathbf{w}_1(n) \\ \vdots \\ \mathbf{w}_L(n) \end{bmatrix}}_{\mathbf{w}(n)}, \quad (7)$$

where $\mathbf{X}_+(n)$ is a block diagonal matrix with L blocks of $\mathbf{X}(n)$, then (5) can be represented as

$$\mathbf{e}(n) = \mathbf{d}(n) + \mathbf{S}^{\mathrm{T}}\mathbf{X}_+(n)\,\mathbf{w}(n). \quad (8)$$

Further, let $\mathbf{F}(n) = \mathbf{X}_+^{\mathrm{T}}(n)\,\mathbf{S}$ represent the filtered reference signal matrix. Note that $\mathbf{F}(n)$ is the combination of $\mathbf{F}(n-1)$ and the latest filtered reference signal at the time index n. Equation (8) can then be represented by

$$\mathbf{e}(n) = \mathbf{d}(n) + \mathbf{F}^{\mathrm{T}}(n)\,\mathbf{w}(n). \quad (9)$$

B. The Proposed Error Weighting Method and Its Application in FxLMS

The proposed error weighting method periodically selects and utilizes Q error microphones to estimate the sound pressures at M error microphones. The vector that consists of the n-th error signal of the selected Q error microphones is denoted as $\widehat{\mathbf{e}}(n)$ with a size of $Q \times 1$, and the rest is denoted

as $\breve{\mathbf{e}}(n)$ with a size of $(M-Q)\times 1$. Let $\mathbf{G}$ be the weighting matrix that estimates T sets of $\breve{\mathbf{e}}$ from $\widehat{\mathbf{e}}$ by

$$\mathbf{G}\underbrace{\left[\widehat{\mathbf{e}}(n)\quad\cdots\quad\widehat{\mathbf{e}}(n-T+1)\right]}_{\widehat{\mathbf{E}}(n)}=\underbrace{\left[\breve{\mathbf{e}}(n)\quad\cdots\quad\breve{\mathbf{e}}(n-T+1)\right]}_{\breve{\mathbf{E}}(n)}. \tag{10}$$

Then the weighting matrix is calculated using the least squares method by

$$\mathbf{G}=\breve{\mathbf{E}}(n)\,\widehat{\mathbf{E}}^{\mathrm{T}}(n)\left(\widehat{\mathbf{E}}(n)\,\widehat{\mathbf{E}}^{\mathrm{T}}(n)+\lambda\mathbf{I}\right)^{-1}, \tag{11}$$

where λ is a regularization factor employed to stabilize the inversion of an ill-conditioned matrix, and in this paper it is set as 1×10^{-4}. For each time interval of I, the weighting matrix $\mathbf{G}$ is recalculated based on the data from Q randomly chosen error microphones.

With the weighting method, the cost function would be

$$J=E\left\{\widehat{\mathbf{e}}^{\mathrm{T}}(n)\left(\mathbf{G}^{\mathrm{T}}\mathbf{G}+\mathbf{I}\right)\widehat{\mathbf{e}}(n)\right\}. \tag{12}$$

Letting $\mathbf{Y}=\mathbf{G}^{\mathrm{T}}\mathbf{G}+\mathbf{I}$, the cost function becomes

$$J=E\left\{\widehat{\mathbf{e}}^{\mathrm{T}}(n)\,\mathbf{Y}\widehat{\mathbf{e}}(n)\right\}. \tag{13}$$

The selected signals and channels are denoted by $\widehat{\mathbf{d}}(n),\widehat{\mathbf{S}},\widehat{\mathbf{X}}_{+}(n),\widehat{\mathbf{F}}(n)$, then similar to (8), we have

$$\widehat{\mathbf{e}}(n)=\widehat{\mathbf{d}}(n)+\widehat{\mathbf{F}}^{\mathrm{T}}(n)\,\mathbf{w}(n). \tag{14}$$

We use the stochastic gradient descent method to minimize the cost function. Introducing (14) to the cost function, the instantaneous gradient of the cost function with respect to $\mathbf{w}$ is

$$\frac{\partial E\left\{\widehat{\mathbf{e}}^{\mathrm{T}}(n)\,\mathbf{Y}\widehat{\mathbf{e}}(n)\right\}}{\partial\mathbf{w}}\approx 2\widehat{\mathbf{F}}\mathbf{Y}\widehat{\mathbf{e}}(n). \tag{15}$$

The control filter $\mathbf{w}$ is then updated with

$$\mathbf{w}(n+1)=\mathbf{w}(n)-2\mu\widehat{\mathbf{F}}\mathbf{Y}\widehat{\mathbf{e}}(n), \tag{16}$$

where μ is the step-size.

The proposed method is termed error weighting FxLMS (EWFxLMS) in this paper, and it is summarized in Table I. The weighting matrix $\mathbf{G}$ is updated every time interval of I with the latest T data samples from Q randomly chosen error microphones. The control filters are updated using the weighting matrix, the filtered reference signal, and the Q error signals.

C. Computation Complexity Comparison

Multiplications constitute the primary computational complexity, so the number of multiplications for every update is summarized in Table II. Additionally, for every time interval of I, EWFxLMS computes every element of $\widehat{\mathbf{F}}(n)$, the weighting matrix $\mathbf{G}$ in Eq. (15), and $\mathbf{Y}$. The extra multiplications for EWFxLMS are summarized in Table III, where the inversion of a Q matrix is assigned a complexity of Q^3 operations. The average extra computation is $(NLQJ+TQ^2+MTQ+MQ^2)/I$ for every update.

TABLE I
EWFXLMS ALGORITHM

Initialize **s**, **w** = **0**, **G**=**I**, $Q, I, i=1$
For n=0, 1, ..., do
if i=I do
1. reinitialized i=1 2. randomly select Q microphones 3. update $\mathbf{G}$ with (11) and let $\mathbf{Y}=\mathbf{G}^{\mathrm{T}}\mathbf{G}+\mathbf{I}$ 4. recompute every element in the filtered-reference signal matrix $\widehat{\mathbf{F}}(n)$ for the recently selected Q microphones
else do
1. $i=i+1$ 2. compute the latest filtered reference signal for the selected Q microphones and form the filtered-reference signal matrix $\widehat{\mathbf{F}}(n)$
update the control filter with (16)

TABLE II
MULTIPLICATIONS FOR EVERY UPDATE

Algorithm	update $\widehat{\mathbf{F}}(n)$	update **w**
FxLMS	MLJ	NLM
EWFxLMS	QLJ	$NLQ+QQ$

When $I=1000, N=J=256, L=6, M=25$, and $T=20$, FxLMS requires 76800 multiplications per update. In contrast, the multiplication of EWFxLMS for varying Q and the corresponding computation savings are summarized in Table IV. Table IV demonstrates that EWFxLMS achieves substantial computational savings.

III. NUMERICAL SIMULATIONS

The transfer functions are generated using the image model [26]. The room dimension is 4 m × 4 m × 4 m, the reverberation time is 0.25 s, the sampling rate is 2 kHz, and the order of the impulse responses and the control filters is 256. Both microphones and loudspeakers are positioned on a plane with a height of 2 m. Twenty-five microphones are arranged in a 5 × 5 grid with a spacing of 5 cm, centered at (1.8 m, 1.2 m, 2 m) as shown in Fig. 2. The reference signal is assumed to be perfectly captured from the white noise source placed at (3 m, 3.5 m, 2 m), which is a white random noise with a band of 0-1000 Hz. Six secondary sources are placed at equal intervals along a line between (1.6 m, 2 m, 2 m) and (2.6 m, 2 m, 2 m). To sum up, in the simulation $N=J=256, L=6, M=25$, and we set $I=1000, T=20$. The maximum step-size for both the FxLMS and EWFxLMS algorithms is approximately 0.02.

The total residual noise level compared to the original disturbances at time n is defined as

$$10\lg\left(\sum_{m=1}^{M}e_m^2(n)\Big/\sum_{m=1}^{M}d_m^2(n)\right). \tag{17}$$

With this definition, the total convergence curves of Q=1, 2, 4, 6 and their comparison to FxLMS are shown in Fig. 3. The figure shows that as Q increases, the convergence curve of EWFxLMS approaches that of FxLMS. When Q=6,

TABLE III
EXTRA MULTIPLICATIONS FOR EWFXLMS

Content	number of multiplication
Compute $\widehat{\mathbf{F}}(n)$	$NLQJ$
Compute $\mathbf{G}$ with (11)	$Q^3 + TQ^2 + MTQ$
$\mathbf{Y} = \mathbf{G}^{\mathrm{T}}\mathbf{G} + \mathbf{I}$	$(M-Q) \times Q^2$

TABLE IV
NUMBER OF MULTIPLICATIONS FOR EWFXLMS PER UPDATE

Q	1	2	4	6	8	10
Multiplications	3467	6936	13880	20832	27793	34762
Saved computation	95%	91%	82%	73%	64%	55%

TABLE V
TOTAL NOISE REDUCTION LEVEL OF EWFXLMS FOR VARYING Q

Q	1	2	4	6	8	10
Noise reduction (dB)	11.44	11.98	12.35	12.55	12.60	12.68
Degradation (dB)	1.50	0.96	0.59	0.39	0.34	0.26

TABLE VI
NOISE REDUCTIONS OF FXLMS AT EVERY MICROPHONE

10.10	13.04	12.77	12.91	10.05
12.65	17.12	14.91	16.75	14.22
12.13	16.96	15.32	15.21	11.88
11.71	17.70	16.67	16.16	10.99
11.75	13.00	11.81	12.06	9.63

TABLE VII
NOISE REDUCTIONS OF EWFXLMS AT EVERY MICROPHONE WHEN Q=1

8.30	10.81	11.56	11.38	8.17
10.98	15.48	16.00	16.93	11.98
11.16	17.26	18.43	16.58	10.89
10.52	15.86	17.35	14.56	9.13
10.13	10.94	10.23	9.63	7.06

the convergence curve of EWFxLMS closely matches that of FxLMS.

The total noise reduction level after convergence is defined as

$$10\lg\left(E\left[\sum_{m=1}^{M} d_m^2(n)\right] \Big/ E\left[\sum_{m=1}^{M} e_m^2(n)\right]\right), \qquad (18)$$

where the symbol E denotes the average of the last 1×10^4 samples. The total noise reduction achieved by FxLMS is 12.94 dB, and the total noise reduction level of EWFxLMS with different Q and degradation relative to FxLMS are summarized in Table V. It can be concluded from Table V that as Q increases, the degradation decreases.

The noise reduction levels (in dB) obtained with FxLMS and EWFxLMS (Q=1) are summarized in Tables VI and VII. The result shows that EWFxLMS achieves a global noise reduction performance comparable to that of FxLMS.

IV. CONCLUSIONS

This paper presents a spatial correlation-based error weighting method for estimating all errors using a subset of error microphones. The weighting method is combined with FxLMS to reduce the number of microphones used in the real-time operation of a multichannel ANC system. The proposed

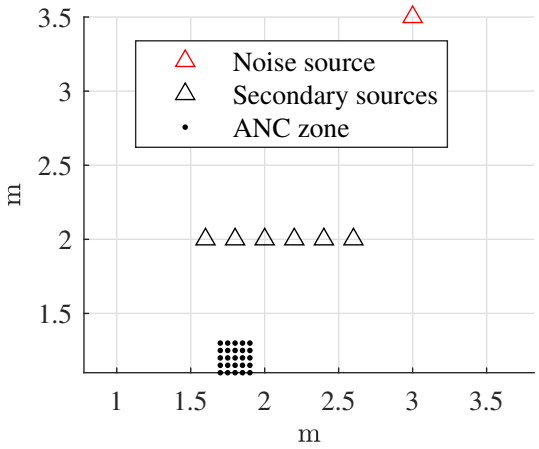

Fig. 2. Illustration of the simulation setup.

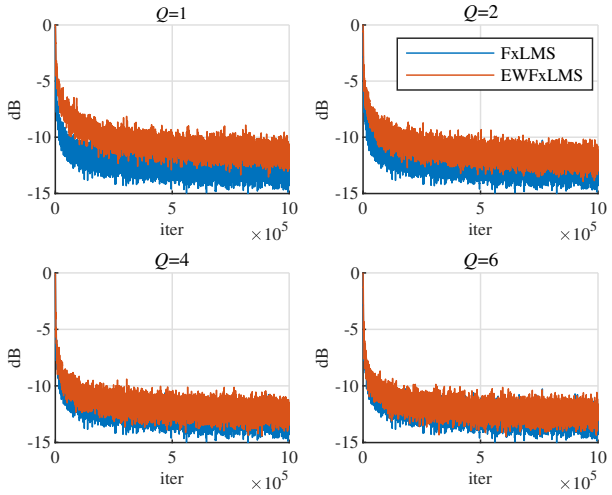

Fig. 3. The total residual noise convergence curves of FxLMS and EWFxLMS for different Q.

algorithm achieves significant computational savings while maintaining competitive global noise reduction performance. Future work will explore the applicability and robustness of the proposed method under larger microphone spacings, and the relationship between error microphone spacing and the selection of the number of active error microphones.

V. ACKNOWLEDGMENT

The authors are sincerely grateful to the anonymous reviewers whose comments helped to improve the quality of this paper.

REFERENCES

[1] P. N. Samarasinghe, W. Zhang, and T. D. Abhayapala, "Recent Advances in Active Noise Control Inside Automobile Cabins: Toward quieter cars," *IEEE Signal Processing Magazine*, vol. 33, no. 6, pp. 61–73, Nov. 2016. DOI: 10.1109/MSP.2016.2601942.

[2] J. K. A. Tan and S.-K. Lau, "Experimental study of active noise control for a full-scale plenum window in a domestic apartment," *Applied Acoustics*, vol. 224, p. 110 120, Sep. 2024.

[3] S. J. Elliott, *Signal Processing for Active Control*. Academic, 2001.

[4] D. Shi, B. Lam, J. Ji, X. Shen, C. K. Lai, and W.-S. Gan, "Computation-efficient solution for fully-connected active noise control window: Analysis and implementation of multichannel adjoint least mean square algorithm," *Mechanical Systems and Signal Processing*, vol. 199, p. 110 444, Sep. 2023.

[5] F. Yang, Y. Cao, M. Wu, F. Albu, and J. Yang, "Frequency-domain filtered-x LMS algorithms for active noise control: A review and new insights," *Applied Sciences*, vol. 8, no. 11, p. 2313, Nov. 2018.

[6] Y. Gao, G. Yu, and M. Gao, "A simplified frequency-domain feedback active noise control algorithm," *Applied Sciences*, vol. 14, no. 7, p. 3084, Jan. 2024.

[7] S. Gaiotto, A. Laudani, G. M. Lozito, and F. Riganti Fulginei, "A computationally efficient algorithm for feedforward active noise control systems," *Electronics*, vol. 9, no. 9, p. 1504, Sep. 2020.

[8] S. Elliott and C. Boucher, "Interaction between multiple feedforward active control systems," *IEEE Transactions on Speech and Audio Processing*, vol. 2, no. 4, pp. 521–530, Oct. 1994.

[9] G. Zhang, J. Tao, X. Qiu, and I. Burnett, "Decentralized Two-Channel Active Noise Control for Single Frequency by Shaping Matrix Eigenvalues," *IEEE/ACM Transactions on Audio, Speech, and Language Processing*, vol. 27, no. 1, pp. 44–52, Jan. 2019.

[10] S. Pradhan, G. Zhang, and X. Qiu, "A time domain decentralized algorithm for two channel active noise control," *The Journal of the Acoustical Society of America*, vol. 147, no. 6, pp. 3808–3813, Jun. 2020.

[11] T. Li, S. Lian, S. Zhao, J. Lu, and I. S. Burnett, "Distributed Active Noise Control Based on an Augmented Diffusion F x LMS Algorithm," *IEEE/ACM Transactions on Audio, Speech, and Language Processing*, vol. 31, pp. 1449–1463, Mar. 2023.

[12] T. Li, S. Zhao, L. Rao, *et al.*, "Experimental study of a distributed active noise control system with multi-device nodes based on augmented diffusion strategy," *The Journal of the Acoustical Society of America*, vol. 156, no. 5, pp. 3246–3259, Nov. 2024.

[13] M. Kamaldar and J. B. Hoagg, "Centralized and decentralized adaptive harmonic control for sinusoidal disturbance rejection," *Control Engineering Practice*, vol. 112, p. 104 814, Jul. 2021.

[14] E. Leboucher, P. Micheau, A. Berry, and A. L'Espérance, "A stability analysis of a decentralized adaptive feedback active control system of sinusoidal sound in free space," *The Journal of the Acoustical Society of America*, vol. 111, no. 1, pp. 189–199, Jan. 2002.

[15] S. Pradhan, G. Zhang, S. Zhao, K. Niwa, and W. Bastiaan Kleijn, "On eigenvalue shaping for two-channel decentralized active noise control systems," *Applied Acoustics*, vol. 205, p. 109 260, Mar. 2023.

[16] Y. Chu, M. Wu, H. Sun, J. Yang, and M. Chen, "Some practical acoustic design and typical control strategies for multichannel active noise control," *Applied Sciences*, vol. 12, no. 4, p. 2244, Jan. 2022.

[17] M. Ferrer, M. de Diego, G. Piñero, and A. Gonzalez, "Active noise control over adaptive distributed networks," *Signal Processing*, vol. 107, pp. 82–95, Feb. 2015.

[18] M. Ferrer, A. Gonzalez, M. de Diego, and G. Piñero, "Distributed affine projection algorithm over acoustically coupled sensor networks," *IEEE Transactions on Signal Processing*, vol. 65, no. 24, pp. 6423–6434, Dec. 2017.

[19] Y. J. Chu, C. M. Mak, Y. Zhao, S. C. Chan, and M. Wu, "Performance analysis of a diffusion control method for ANC systems and the network design," *Journal of Sound and Vibration*, vol. 475, p. 115 273, Jun. 2020.

[20] K. Mazur, S. Wrona, A. Chrapońska, J. Rzepecki, and M. Pawełczyk, "FXLMS with multiple error switching for active noise-cancelling casings," *Archives of Acoustics*, vol. 44, no. 4, pp. 775–782, Nov. 2019.

[21] M. Hu, H. Li, J. Lu, H. Zou, and Q. Ma, "An online modeling virtual sensing technique based on kriging interpolation for active noise control," *Mechanical Systems and Signal Processing*, vol. 224, p. 112 186, Feb. 2025.

[22] S. Koyama, J. Brunnstrom, H. Ito, N. Ueno, and H. Saruwatari, "Spatial Active Noise Control Based on Kernel Interpolation of Sound Field," *IEEE/ACM Transactions on Audio, Speech, and Language Processing*, vol. 29, pp. 3052–3063, Aug. 2021.

[23] S. J. Elliott, P. Joseph, $.Bullmore$, and P. A. Nelson, "Active cancellation at a point in a pure tone diffuse sound field," *Journal of sound and vibration*, vol. 120, no. 1, pp. 183–189, Jan. 1988.

[24] D. J. Moreau, J. Ghan, B. S. Cazzolato, and A. C. Zander, "Active noise control in a pure tone diffuse sound field using virtual sensing," *The Journal of the Acoustical Society of America*, vol. 125, no. 6, pp. 3742–3755, Jun. 2009.

[25] B. Rafaely, "Spatial-temporal correlation of a diffuse sound field," *The Journal of the Acoustical Society of America*, vol. 107, no. 6, pp. 3254–3258, Jun. 2000.

[26] E. A. Habets, "Room impulse response generator," *Technische Universiteit Eindhoven, Tech. Rep*, vol. 2, no. 2.4, p. 1, May 2006.